

2006

Thermo-elastic detection of heat damage in composites

John Thomas Welter
University of Dayton

Follow this and additional works at: https://ecommons.udayton.edu/graduate_theses

Recommended Citation

Welter, John Thomas, "Thermo-elastic detection of heat damage in composites" (2006). *Graduate Theses and Dissertations*. 6310.

https://ecommons.udayton.edu/graduate_theses/6310

This Thesis is brought to you for free and open access by the Theses and Dissertations at eCommons. It has been accepted for inclusion in Graduate Theses and Dissertations by an authorized administrator of eCommons. For more information, please contact mschlange1@udayton.edu, ecommons@udayton.edu.

THERMO-ELASTIC DETECTION OF HEAT DAMAGE IN COMPOSITES

Thesis

Submitted to

The School of Engineering of the
UNIVERSITY OF DAYTON

in Partial Fulfillment of the Requirements for

The Degree

Master of Science in Materials Engineering

by

John Thomas Welter

UNIVERSITY OF DAYTON

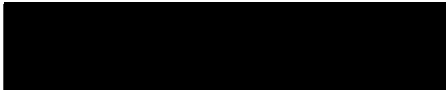
Dayton, Ohio


August, 2006

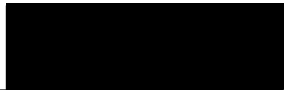
THERMO-ELASTIC DETECTION OF HEAT DAMAGE IN COMPOSITES

APPROVED BY:


Shamachary Sathish, Ph.D.
Advisory Committee Chairman
Assistant Professor
Materials Engineering


P. Terrence Murray, Ph.D.
Committee Member
Professor
Materials Engineering


Mark Blodgett, Ph.D.
Committee Member
Senior Materials Engineer
AFRL Materials and Manufacturing Directorate


Donald L. Moon, Ph.D.
Associate Dean
Graduate Engineering Programs
and Research
School of Engineering


Joseph Saliba, Ph.D., P.E.
Dean
School of Engineering

ABSTRACT

THERMO-ELASTIC DETECTION OF HEAT DAMAGE IN COMPOSITES

John Thomas Welter
University of Dayton

Advisor: Dr. Shamachary Sathish

Heat damage of polymer matrix composites (PMCs) caused by heat exposure that exceeds design specifications can dramatically degrade the strength of these materials. This type of damage can result from lightning strikes, fires, exhaust wash, maintenance and repair mishaps, etc. Destructive measurements of overheated PMCs have shown that their mechanical strength can be reduced by as much as 10-80 percent before there is visible damage. Traditional nondestructive evaluation (NDE) techniques are only successful in detecting severely damaged regions such as ply delaminations and matrix cracking. A large majority of the NDE techniques cannot detect incipient damage in PMCs and typically measure only changes to a single material property. This thesis presents an NDE method that measures the thermo-elastic parameter of the material. Results from this evaluation demonstrate the feasibility of detecting incipient heat damage in PMCs by comparing the thermo-elastic parameter measured in pristine samples and samples damaged by controlled heat

exposure. Thermo-elastic measurements are compared with ultrasonic C-scan from the same set of specimens. These measurements confirm that the traditional measurement technique cannot detect heat damage that can be detected by the thermo-elastic parameter measurements. In addition, experimental details of the thermo-elastic parameter measurements and possible mechanisms responsible for the change in this parameter due to heat damage are discussed. A gradual decrease in the thermo-elastic parameter is determined as a function of increasing time of exposure at a constant temperature. The change in thermo-elastic measurements are compared with destructive flexural strength measurements performed on the sample. The results of these measurements indicate that this technique may be a viable tool for detecting heat damage in composite structures.

ACKNOWLEDGMENTS

First I would like to acknowledge the Air Force Research Laboratory's NDE Branch for their support of this work; without them this would not have been possible. I would like to thank my advisor Shamachary Sathish. He was instrumental in helping me interpret the data and understand the physical meaning behind it. I would also like to thank Charles Buynak for allowing the use of the Four Powers sample, Erik Ripberger and MLSA for providing composite samples, Richard Reibel for his help in troubleshooting the electronics, the air coupled ultrasonic C-scans of the Four Powers panel, and the IR camera calibration, Nicholas Kreitingner for providing the ultrasonic C-scans of the MLSA panels, and Eric Lindgren and Kumar Jata for their advice and counsel.

A special thanks goes to my all my family and friends for helping and encouraging me. Lastly I would like to thank my fiancée, Stephanie Lynn Munday, for her loving kindness and patient encouragement through it all.

TABLE OF CONTENTS

ABSTRACT	iii
ACKNOWLEDGEMENTS	v
LIST OF FIGURES.....	ix
LIST OF TABLES	xi
CHAPTER	
I. INTRODUCTION.....	1
A. Motivation	1
B. Polymer Matrix Composites	4
C. Review of Nondestructive Evaluation Techniques	6
i. Shearography.....	7
ii. Hardness Testing	8
iii. Glass Transition Temperature	9
iv. Microwave	9
v. Eddy Current	10
vi. Composite Analyzer Tester	11
vii. Ultrasonic C-scan	11
viii. Leaky Lamb Waves	12
ix. Compton Scattering.....	13

x. Gamma and Neutron Radiation.....	13
xi. Laser Pumped Fluorescence.....	14
xii. Diffuse Reflectance Infrared Fourier Transform Spectroscopy	14
xiii. Infrared Thermography	15
xiv. Microwave Thermography	16
xv. Vibrothermography and Related Methods	16
II. METHOD AND INSTRUMENTATION.....	17
A. Vibrothermography.....	17
B. Stress Pattern Analysis by Thermal Emission	19
C. Sonic IR	21
D. Non-contact Thermo-elastic Damage Detection.....	22
i. Acoustic Displacement Measurements	26
ii. Temperature Increase Measurements.....	28
III. COMPOSITE SAMPLES AND HEAT DAMAGE	32
A. Four Powers Sample.....	32
B. MLSA Samples.....	36
IV. RESULTS AND DISCUSSION.....	38
A. Ultrasonic C-scan Imaging	38
i. Four Powers Sample.....	39
ii. MLSA Samples.....	40

B. Non-contact Thermo-elastic Measurements.....	42
i. Four Powers Sample.....	43
ii. MLSA Samples.....	46
C. Discussion.....	50
A. Conclusions	56
B. Future Work.....	57
REFERENCES.....	60

LIST OF FIGURES

1: Non-contact Thermo-elastic Materials Damage Test Set Up.....	23
2: Ultrasonic Horn Stack.....	24
3: Fiber Optic Displacement Sensor.....	27
4: Diagram of Displacement Measurements.....	28
5: IR Camera Calibration Curve.....	29
6: Diagram of Temperature Measurements.....	31
7: Four Powers Sample Exposed/Unpainted Side.....	35
8: Four Powers Sample Unexposed/Painted Side.....	35
9: MLSA Panels Front/IR Camera Side	37
10: MLSA Panels Back/Ultrasonic Horn Side	37
11: UT C-Scan Image: Four Powers Sample Exposed/Unpainted Side	39
12: UT C-Scan Image: Four Powers Sample Unexposed/Painted Side	40
13: UT C-Scan Image: MLSA Panel 11-5-P1-D.....	41
14: UT C-Scan Image: MLSA Panel 11-5-P2-D.....	42
15: Four Powers Sample - Average Temperature Rise vs. Amplitude.....	44
16: Four Powers Sample - Average Displacement vs. Amplitude.....	44
17: Four Powers Sample Average Temperature Rise vs. Average Displacement	45

18: Four Powers Sample Average Temperature Rise vs. Average

Displacement for Varying Amounts of Heat Damage 45

19: MLSA 11-5-P1-D: All Locations Average - Temperature Rise vs. Average

Displacement 47

20: MLSA 11-5-P2-D: All Locations Average - Temperature Rise vs. Average

Displacement 48

LIST OF TABLES

Table 1: Four Powers Sample Heat Exposure Data	33
Table 2: Four Powers Sample: Comparison of χ^2 Coefficients	46
Table 3: MLSA Samples: Comparison of χ^2 Coefficients	50

CHAPTER 1

INTRODUCTION

Motivation

Recently polymer matrix composites (PMCs) have enjoyed a great increase in number of applications using their unique properties. Many of these applications are in the aerospace industry where demands for performance and reliability dictate the use of lightweight materials that have superior strength and reliability [1]. There are also composite applications in other industries, for example composites are used in rail cars, sports equipment, civil structures, marine craft and automobiles [2, 3].

In modern commercial as well as military aircraft a significant portion of the weight is made of composites. Commercial aircraft such as the Airbus 340, Boeing 747 and 777 composites account for 5-10% of their structural weight and another 80-90% of the cabin furnishings. Composite structure in next generation commercial aircraft such as the Boeing 787 or the Airbus A380 is expected to exceed 20% [4]. In current military aircraft like the French Rafale, European Fighter Aircraft (EFA), Indian Light Combat Aircraft (LCA), or Swedish JAS-39 approximately one-third of the structure is already polymer matrix composite [1].

The V-22 Osprey has an entirely composite wing with 72% of the total aircraft weight being either carbon or glass reinforced polymer. Soutis hypothesizes that in the future more than 50% of the structural mass of aircraft will be a fiber reinforced polymer composite of one form or another [5]. Clearly, the use of PMCs is expected only to increase in the near future.

Increasing use of composites brings with it new challenges and one of these challenges is different damage mechanisms when compared to metals. It is widely known that composites can suffer from impact damage that causes cracking and delaminations that reduce the physical properties of the structure. This is in addition to cracking and delaminations induced through normal use and possibly abuse such as over loading. Composites with organic components, such as carbon fiber epoxy composites, are susceptible to heat damage which does not have a significant effect on traditional aerospace metals. Sources point out that heat induced damage can result in a dramatic reduction in strength [6]. Heat damage can be defined as a heat exposure that exceeds the design specifications of the composite. This can be a result of fire, lightning strikes, heating blankets (used in repair of composite on aircraft), exhaust impingement from missiles or engines, and similar accidental exposures [6]. Anecdotal evidence suggests repairs that generate thermal energy, such as welding or grinding on metal structure that neighbor's composite structure, can be a source of heat damage to composites when proper safeguards are not taken.

Of particular concern is a type of heat damage called incipient heat damage. This is an over temperature event that causes a severe reduction in composite strength without causing cracking or delamination. Gross damage, i.e. cracking and delaminations, in composites can be detected easily by several different NDE methods. However incipient heat damage cannot be detected by conventional methods. This type of heat damage is not detectable by ultrasonic methods, which are the current methods used in the aircraft maintenance industry to detect areas of composite with heat damage that resulted in cracking and delaminations [7]. Matzkanin shows that numerous other NDE techniques have been tried and are largely ineffective [8]. Only glass transition temperature, laser pumped fluorescence and diffuse reflectance IR Fourier transform spectroscopy, and microwave thermography appear to be able to detect incipient heat damage to some degree [8]. Each of these techniques has advantages and drawbacks that will be discussed later in this chapter. A review of the literature indicates that none of these techniques are in use at present for incipient heat damage detection. This poses a problem for commercial and military aircraft maintainers that are required to inspect aircraft for airworthiness at periodic intervals, and must have accurate and reliable tools and techniques to perform those inspections.

The primary goal of this thesis is to develop a nondestructive evaluation technique that will enable the inspection of polymer matrix composites for

damage induced by exposure to heat in excess of the materials service temperature. This system uses a combination of a temperature measurement and a mechanical vibration measurement in a sample under ultrasonic excitation. This combined response is a unique combination of material properties called a thermo-elastic parameter. This parameter for an undamaged sample is compared to the parameter for a heat damaged sample. Study of different amounts of heat damage to a PMC and the corresponding thermo-elastic response is performed.

To better understand the problem space a brief introduction to polymer matrix composites is provided in this chapter. This is followed by a review of NDE methods that have been evaluated previously for detection of incipient heat damage in composites. NDE methods that are similar in form and methodology to the technique developed here are discussed in Chapter 2.

Polymer Matrix Composites

Polymer matrix composites are materials that consist of fibers that are held together with a matrix, which is typically an epoxy resin. The reinforcing fiber could be either continuous (long fibers that run throughout the composite) or discontinuous (short pieces of fiber in comparison to the length of the composite). The fibers are usually glass or carbon. PMCs have many advantages. The polymer matrix enables PMCs to be easily formed, while the fibers instill a great

increase in strength compared to the neat resin (polymer resin without reinforcing fibers) [2].

The strength of a PMC is a combination of the fiber and matrix strengths based on the volume fractions of the matrix and the fibers [2]. However, the use temperature of a PMC is based primarily on the use temperature of the resin in the matrix. It is clear through experiments in graphite-epoxy composites, that all other mechanical integrity is lost sometime before the fiber shows a reduction in properties such as tensile strength. The fibers in a PMC carry the majority of the tensile load and they degrade more slowly under heat exposure than the matrix resin. This makes tensile strength a poor indicator of incipient heat damage. PMC mechanical properties that are greatly affected by heat damage and therefore the ones that are the most sensitive to it include the compressive, shear and flexural properties. Material properties are also impacted, and include glass transition temperature, thermal expansion coefficient, thermal conductivity and heat capacity [9].

Previous work has been performed in heat damage studies on a variety of composite systems with various fiber and matrix combinations. The common denominator in these studies is that once the composite is exposed to temperatures exceeding the use temperature of the resin, the resin begins to break down. This severely degrades the mechanical properties of the composite [7, 8, 10, 11]. One explanation on how heat damage evolves in composites is

from the Naval Air Warfare Center, Aircraft Division [12]. Incipient damage is induced at lower over temperature and longer time exposures. It is also more of a concern in dry to ambient humidity conditions. This is in contrast to lamination plane cracking that is induced by internal pressure from volatiles and trapped moisture, and which is more prevalent at higher over temperature exposures [12].

The amount of degradation in mechanical properties before there is a visual indication of damage can be up to 40% according to one source [13] and between 10-80% according to another [14]. This difference could possibly be attributed to the method of heat exposure, radiant lamp versus fuel fire, between the two studies or the intensity of the heating source since both studies used the same matrix resin. Given the most conservative figure of 10%, it is clear that this type of heat damage must be detected in order to prevent the in-service and potentially fatal failure of heat damaged composites.

Review of Nondestructive Evaluation Techniques

Review of the literature shows that the NDE methods used for composite material inspection that also showed promise initially for incipient heat damage detection usually comprised well established techniques that were developed to detect discrete flaws. These techniques could typically be categorized in one of the following five areas: thermal/IR, radiographic, dielectric properties, or

ultrasonic. A drawback of these techniques is that these traditional methods are incapable or limited in their ability to detect the minute property changes that occur before the mechanical properties begin to degrade [8]. Recent advances show that laser pumped fluorescence, LPF (also known as laser induced fluorescence, LIF), and diffuse reflectance infrared Fourier transform spectroscopy (DRIFT or DRIFTS) show encouraging results to detect heat damage.

The following is an extensive review of the current NDE techniques and their applicability for detection of incipient heat damage. Much of the data on the effectiveness of these techniques to detect incipient heat damage in composites is from a program conducted by the Grumman Aerospace Corp. for the Great Lakes Composite Consortium (GLCC). It was coordinated with Grumman Aerospace, McDonnell Douglas Aerospace, Oak Ridge National Laboratory (ONRL) and the Naval Air Warfare Center (NAWC) in Warminster. This data is included as referenced in Matzkanin [8] and will be referred to here as the GLCC Study.

Shearography

Shearography is a NDE method that is typically used to detect disbonds, delaminations and other material discontinuities. It is developed as an interferometric strain measurement technique. Shearography utilizes a laser and

optics to perform a full field inspection that detects the presence of discontinuities by the induced strain concentrations they create. It should be noted that while shearography is a surface measurement technique it can also detect internal defects that affect the surface deformation. This is basically a non-contact technique. However, stresses must be applied to the test object to generate the strain pattern [15]. The GLCC Study finds this to be ineffective at detecting incipient heat damage [8].

17

Hardness Testing

Hardness testing is a method of measuring the resistance of a sample to surface indentation or abrasion. Hardness is not defined by an absolute scale and as such each hardness test has its own arbitrarily defined hardness values [16]. This method is not strictly nondestructive in that it does leave a small indent or scratch on the sample. Several groups have tried to use hardness testing by different methods to detect heat damage and they all have shown some trends in hardness fall off with damage. It is ineffective at detecting heat damage before significant strength loss has occurred [6, 8, 17].

Glass Transition Temperature

Glass transition temperature (T_g) is studied to measure changes caused by heat damage in composites. Measurement of T_g is performed by removing a small piece of composite from an area to be measured and using a thermomechanical analyzer [18]. It is shown that the T_g decreases with heat exposure and this correlates to a decrease in mechanical properties. However this method is not strictly nondestructive since a small amount of material must be removed from the region to be inspected. This is not an issue if the area is under no load, but it becomes a concern when the part involves load bearing structure where removing a small section of material can generate a stress concentration that can lead to other damage [19].

Microwave

Microwave nondestructive evaluation describes a wide range of techniques that use electromagnetic waves in the 300-1,000,000MHz range. Reflection and refraction of microwaves is very similar to light. However, the defect size that can be resolved is limited in simple microwave techniques to the wavelength of microwave used. Some of the most common microwave techniques include transmission (fixed and swept frequency continuous wave, pulse modulated), reflection (fixed and swept frequency continuous wave, pulse modulated), swept

wavelength continuous wave, fixed-frequency (standing waves and scattering) [20].

Some advantages of microwave techniques are their ability to propagate through empty space and that they are not totally reflected by a solid-air interface. Disadvantages include the inability to penetrate conductive materials to any significant depth and alignment of the waveguides and detectors is often quite complicated [20]. The GLCC Study finds microwave to be ineffective at detecting incipient heat damage in composites [8].

Eddy Current

Eddy currents are defined as currents that flow in a conductor as a result of the influence of a time or space varying magnetic field. In a typical inspection a coil with an alternating current passing through it is placed in close proximity to a conductive sample. The current in the coil induces a magnetic field in the sample. This magnetic field induces an opposite current back into the coil. Sample material properties as well as sample discontinuities affect the magnitude and phase of the induced current. It is these changes that can be measured and used to assess a materials condition [20]. Eddy current is found to be ineffective at detecting incipient heat damage in the GLCC Study [8].

Composite Analyzer Tester

The composite analyzer tester, CAT, is a NDE tool that uses both ultrasonic and eddy current to probe a material. It can determine the thickness of a graphite epoxy composite by magnetic/inductive energy, and then uses that data to measure the velocity of ultrasound in the composite. Relative ultrasonic attenuation, relative conductivity, and if material properties are known an estimate of strength is also possible [21]. The CAT is ineffective for incipient damage detection [8].

Ultrasonic C-scan

Ultrasonic C-scan is a method of scanning an ultrasonic transducer over a part and recording the signal at each point to build an image. This is analogous to taking an A-scan (one point ultrasonic measurement at every point) or a series of B-scans (a line of A-scans) along an area of a part. Pulse-echo (one transducer sends out a signal and that same transducer receives the signal after it interacts with the sample) or pitch-catch (one transducer sends out a signal and a different transducer receives the signal after passing through or reflecting off of the sample) methods of ultrasonics can be used depending on the application or sample. Typically the transducer(s) are scanned by computer controlled motors for C-scan imaging [20]. Ultrasonic C-scan imaging is shown numerous times to

be effective at detecting disbonds and delaminations in heat damaged composites, but is shown to be ineffective at detecting incipient heat damage [7, 8, 11, 17]. Even heat damage that induces cracking and delaminations is sometimes difficult to quantify with ultrasound. Superficial or surface damage areas can appear in ultrasonic imaging as severely damaged regions while the composite shows little to no reduction in strength [10]. Other ultrasonic based techniques that are shown to be ineffective at detecting incipient heat damage are resonance ultrasound and resonant ultrasound spectroscopy [8].

Leaky Lamb Waves

Leaky Lamb waves are waves that "leak" into the fluid surrounding a plate that is being excited by a guided wave while immersed in a fluid. Investigations performed on carbon epoxy composite showed that backscattered strength of leaky Lamb waves could be used as an indicator of heat damage in the first surface ply and has the advantage of being a one sided inspection using only one transducer. Deeper heat damage could be then determined with a full thickness leaky Lamb wave technique, although this would be sensitive to any change in thickness [14]. It is reported that changes in stiffness of composites as a result of heat damage could be detected with leaky Lamb waves [8]. Overall leaky Lamb wave results show that it may be possible to detect incipient heat damage [8, 14].

Compton Scattering

Compton scattering is an x-ray based technique that utilizes Compton (backscattered) x-rays from low atomic number samples to generate contrast based on the mass density of the scatterer. This technique is developing for biomedical applications, but it is finding some applications in NDE as well. One advantage is that it requires access to only one side of the sample [22]. However, this is negated by requiring the use of an x-ray source, and detectors, plus proper safety measures must be taken. This technique is shown to be sensitive to changes in density in a composite with heat damage, and the authors of that study suggest that it can be applied to in situ monitoring of composites during fire testing [23]. It is found to be ineffective for incipient heat damage detection according to work done by the GLCC study [8].

Gamma and Neutron Radiation

Gamma and neutron radiation based methods are similar to x-ray methods in that they use ionizing radiation and diffraction techniques. The only difference is the source of the radiation. Gamma radiation is created by radioactive decay while x-rays are created by electrical means for NDE. Neutron radiation in turn comes from a nuclear reactor. Both gamma and neutron radiation can be used for penetrating and scattering methodologies for NDE [20]. The obvious

disadvantage to both of these is the source of radiation. Handling radioactive material or needing to be close to a reactor makes inspection more difficult. However, they are studied and found to be ineffective for incipient heat damage detection [8].

Laser Pumped Fluorescence

Laser pumped fluorescence (LPF) or laser induced fluorescence (LIF) involves using a laser to stimulate the resin molecules at the surface of a PMC. These molecules then fluoresce, releasing part of the absorbed laser energy in the form of light at greater wavelengths. The emission spectra are characteristic of the resin. Therefore the spectra are changed by anything that changes the resin properties such as heat damage [24]. This technique is shown to be effective at detecting incipient heat damage but not at quantifying it [8, 22, 25]. This technique is a surface technique and is not capable of determining through thickness damage. In addition a field system is not demonstrated in the literature, although a field system concept is discussed [24, 25].

Diffuse Reflectance Infrared Fourier Transform Spectroscopy

Diffuse reflectance infrared Fourier transform spectroscopy (DRIFT or DRIFTS) is a spectroscopy method that collects diffusely scattered IR light from a

sample surface. This light is processed to form an IR spectrum from which qualitative and quantitative chemical information can be determined. DRIFT is shown to be sensitive to changes in composites resulting from heat damage [19, 25]. It is described as acceptable for field inspection [25]. Limited field inspections are conducted with promising results. Data is correlated between the DRIFT samples and the flexural test samples under the assumption that the two sets of samples have identical structure. This demonstrates its effectiveness at sizing heat damage. However, the surface must be thoroughly stripped of paint, since even trace amounts of paint will interfere with the technique [8].

Other related spectroscopic techniques that have been tried and that are shown to be ineffective include: attenuated total reflectance (ATR), fluorescence, specular reflectance, Fourier transform – Raman, diffuse reflectance visible (400-700nm), and ultraviolet-visible diffuse reflectance (200-800nm) [25].

Infrared Thermography

Infrared (IR) thermography characterizes the diffusion of thermal energy in a material. Typically this involves the heating or cooling of a test sample by radiative (heat lamp, refrigerated surface, etc.), convective (ovens, blowers, etc.) or conductive (hot/cold plate, etc.) means and recording the resulting thermal gradients. It should be noted that the thermal gradients can be measured during or after sample excitation. Measurement of thermal gradients can be

accomplished through contact means (temperature sensitive paints, phosphors, papers, etc.) or by non-contacting means (IR video or still camera, etc.) [20]. IR thermography is capable of detecting impact damage in graphite-epoxy composites [15]. However, it fails to detect incipient heat damage in composites [7, 8].

Microwave Thermography

Microwave thermography is a related technique of IR thermography. The only difference is that in microwave thermography the sample is heated by microwaves and the cooling of the sample is recorded by IR camera [26]. This technique is only at the proof of concept stage although it shows promise in detecting incipient heat damage in composites [8].

Vibrothermography and Related Methods

Vibrothermography, stress pattern analysis by thermal emission (SPATE) and sonic IR are all NDE techniques that are closely related to the technique developed here. They are explained in detail in Chapter 2.

CHAPTER 2

METHOD AND INSTRUMENTATION

The NDE techniques of stress pattern analysis by thermal emission (SPATE), vibrothermography, and sonic IR are based on the measurement of the thermo-elastic response of the material. Each of these techniques takes advantage of the mechanical energy input into a material that generates thermal energy, which is recorded and analyzed. In this way they all use the thermo-elastic effect, although each one uses different methods to mechanically excite the thermal emission, to record data, and to analyze data.

Vibrothermography

Vibrothermography is a NDE technique in which mechanical oscillations are induced in a part and the resulting signal created by the transformation of mechanical to thermal energy is recorded. Analysis of the temperature map of the material is used to indicate locations of damage such as cracks and delaminations. These changes could be the result of frictional heating of the faces of a defect or other irreversible thermo-elastic interactions [27].

In vibrothermography mechanical excitation can be applied in a variety of ways to achieve the low amplitude steady-state mechanical vibrations necessary to create thermal signals that can be imaged. Contact excitation is used to generate the mechanical vibration. Fatigue machines, commercial shakers, ultrasonic horns, and a transducer from a glassware cleaner have been used as excitation sources [28]. The frequency of excitation may range from a few Hz to tens of kHz. Thermal signals resulting from the excitation are captured in non-contact with an IR camera. These thermal patterns are analyzed for any discontinuities or aberrations. Typically, this type of inspection takes a few seconds. Discontinuities are indicative of an inhomogeneity in the material that causes a thermal gradient due to a difference in thermal conductivity. Discontinuities are typically cracks, delaminations, and other defects in the part under observation. This method is fast. A thermal pattern showing thermal gradients indicative of a delamination in a composite part typically can be observed in seconds [27]. Previous work describes using a high power ultrasound horn in contact for long periods of time (10s of seconds) to excite heating at resonant nodes as well as grain boundaries and other defects with an IR camera [28]. Since the technique has full field capability, an entire part can be inspected simultaneously. This technique only takes a few seconds to inspect a composite part.

This technique is not without limitations. Vibrothermography does not yield quantitative information about a material defect. It can locate defects and relative sizing of defects is possible. Another drawback is that the part to be inspected must be excited mechanically through direct contact. This limits the in-situ inspection of parts. Surface damage as a result of the mechanical excitation is also a concern.

Stress Pattern Analysis by Thermal Emission

In SPATE a part is cyclically loaded and the temperature change is captured with an IR camera. The frequency of loading is typically between 0.5 Hz and 20 kHz and this can be achieved in a variety of ways. Some examples are shakers, pneumatic actuators and running equipment. The dynamic temperature signal and the reference signal from the loading source are input into a lock-in amplifier. The reference signal is used as a frequency and phase reference for the temperature data in order to reject temperature data that is not related to dynamic stress. In addition the reference signal synchronizes storage of the temperature and stress data. The phase difference between the temperature and reference waveforms across the structure allows differentiation of the regions of the structure under tensile stress from those under compressive stress [15].

The damage is detected by changes in the stress field measurements and damage propagation can be observed in samples under fatigue. Quantitative estimation of damage can be performed with thermo-elastic theoretical calculations even on anisotropic structures. In isotropic materials information on the sum of the principle stresses and in anisotropic materials a weighted combination of stresses along the directions of principle axes of material symmetry can be determined. Stress separation is possible with complex numerical or experimental techniques. SPATE can also be used as a design tool in order to optimize the stress distribution in parts. Due to the non-contact measurement of the IR and reference signal, high temperature measurements are possible [15].

SPATE can be used for full field quantitative measurement and analysis. The drawbacks of the technique include the sample should have a high uniform surface emissivity and some form of dynamic loading must be applied [15]. SPATE methodology is untested at detecting heat damage in composites after review of the literature. Due to its similarity to vibrothermography, with the addition of stress quantification aspect it is reasonable to assume that SPATE would have comparable abilities in detecting heat damage.

Sonic IR

Sonic IR is similar to vibrothermography in use and applications. It uses a short pulse of ultrasonic energy to mechanically excite a part. This excitation causes defects like cracks and delaminations to convert the mechanical energy to thermal energy due to frictional and other irreversible interactions. Heating at defects is imaged by an IR camera [29].

Typically excitation is accomplished by an ultrasonic horn in contact with the part to be inspected. Coupling of the horn to the part is important in order to ensure maximum sound transfer efficiency. A piece of copper sheet can be used to increase sound transmission [29]. An option is to use a sacrificial piece of material with the same acoustic impedance as the material being tested to efficiently transfer the energy from the horn to the part and prevent the horn from damaging the surface of the part being inspected [30]. Different groups are using paper [31] or related materials with successful results [32]. Supporting the part under test is also important and it has been found that cork [33] or gasket type material is beneficial in ensuring the proper excitation and minimizing energy losses to the supporting structure [32, 33]. The usual frequency of excitation is 20 kHz to 40 kHz. An excitation pulse duration of 50 ms to 200 ms is commonly used. This excitation can be applied at any convenient location [29]. Any thermal signals at a defect are recorded by an IR camera. In this method only brief heating from any defects that maybe present is captured [29].

Advantages of this technique include, that it takes only a few seconds to inspect a part and capture the data in the form of a video or series of still images. Data collected shows the defect location, usually as a bright spot, where the heating occurs at the defect due to the mechanical excitation. This simplifies defect detection. Image enhancement techniques, such as background subtraction, can also be applied as needed to increase the signal to noise ratio and enhance defect detection.

One disadvantage of this technique is the potential for surface damage to occur during the excitation of the part by the ultrasonic horn. The need for coupling and supporting media to ensure efficient excitation for an optimized signal is another disadvantage.

Non-contact Thermo-elastic Damage Detection

A major disadvantage common to all of the techniques based on imaging heat generated to due to mechanical excitation is the need for direct contact with the material for excitation. A non-contact excitation technique to introduce the acoustic energy into the materials will be extremely useful for NDE of materials. Such a methodology is described here. The technique is called non-contact thermo-elastic damage detection. It uses a non-contacting mechanical excitation method to generate thermo-elastic heating in a composite. The maximum temperature rise and the displacement of the part caused by the excitation are

measured by non-contacting methods with respect to excitation amplitude.

This enables the temperature increase as a function of acoustic displacement plot to be made. A picture of the experimental set up is shown in Figure 1. Parts of the set up are labeled. Item A is the ultrasonic horn. Item B is the aluminum frame that holds the sample. Item C is the motion stages controlling the sample and fiber optic displacement sensor placement. Item D is the mounting rod for the fiber optic displacement sensor, which is not shown in this figure. Item E is the IR camera.

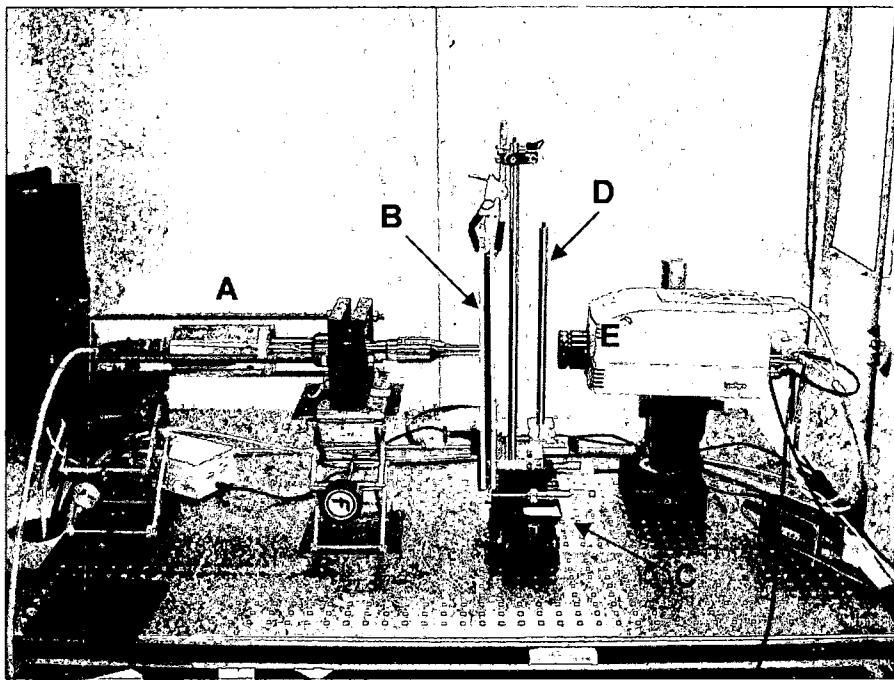


Figure 1: Non-contact Thermo-Elastic Materials Damage Test Set Up

The technique uses a non-contacting high power ultrasonic source. A Branson Model 900BCA power supply is used to supply the power and input

signal to the converter/booster/horn stack (item A in Figure 1 and close up view in Figure 2). The converter (item A in Figure 2) is a series of piezoelectric elements that convert the electrical signal from the power supply to mechanical energy through the piezoelectric effect. The mechanical vibration created in the converter travels to the booster (item B in Figure 2), which as the name implies mechanically amplifies the signal increasing its amplitude. The boosted signal passes into the horn (item C in Figure 2). The horn further amplifies the amplitude of the mechanical signal. The mechanical displacement at the end of the horn is between 70 and 180 microns based on experimental measurements.

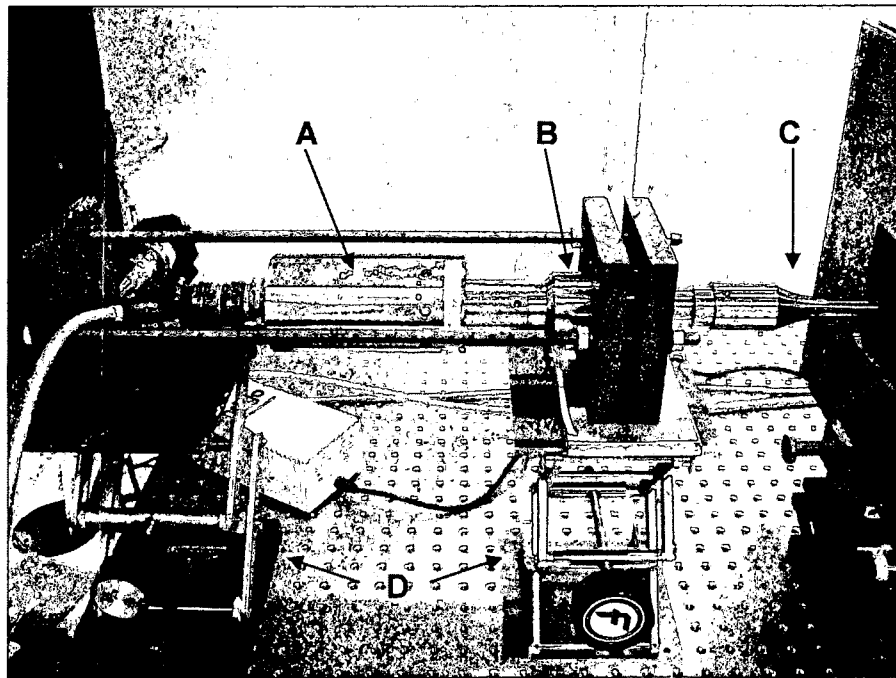


Figure 2: Ultrasonic Horn Stack

The ultrasonic energy propagates a small distance through the air to the sample to be inspected. This distance is approximately 380 microns. This is determined experimentally to be an acceptable standoff distance.

Measurements of the maximum displacement of the horn from minimum to maximum amplitude of the power supply are conducted. The standoff distance of 380 microns is almost twice the displacement of the horn at maximum amplitude, which is less than 180 microns. This is done to ensure that the horn does not contact the part during excitation. Standoff distance should be kept as small as possible to maximize the propagation efficiency of the ultrasonic energy as much as possible and ensure non-contact excitation of the part. In the experimental set up the ultrasonic horn is supported by two lab jacks (item D in Figure 2) to allow it to be centered with respect to the sample holding frame in the vertical direction.

The sample is held tightly in an aluminum frame (item B in Figure 1). The frame is made of two pieces of aluminum that are held together with screws at the four corners. There is a square window cutout in the center of each piece. This allows the horn to be brought close to the sample for excitation on one side and the window on the other side allows measurement of the displacement and temperature change of the composite during inspection. The composite is protected from surface damage by corrugated cardboard gaskets while it is in the frame. The frame is held at the bottom and at the top by laboratory mounting

hardware to two manual motion stages and a lab jack (item C in Figure 1). The position of the vertical support (item D in Figure 1) is controlled by a manual motion stage attached to the two motion stages and lab jack assembly. This support is used for mounting the fiber optic displacement sensor. The fiber optic displacement sensor is used for measuring the out of plane displacement of the sample. The manual motion stages provide course and fine movement to set the standoff distance of the sample and fiber optic displacement sensor from the ultrasonic horn. This allows the fiber optic displacement sensor to be positioned at the proper distance from the sample based on its base voltage output while the sample is not being excited. The lab jack allows movement of the sample and fiber optic in the vertical direction to allow alignment of the ultrasonic horn with the center of the frame window.

Acoustic Displacement Measurements

Acoustic displacement measurements of the part under excitation are performed separately from the temperature measurements. Measurements are performed with a Philtec fiber optic displacement sensor model D20+H1PQ (Figure 3). This sensor is a photonic displacement sensor that measures out of plane displacements by emitting light and measuring changes in the light intensity reflected from a surface. The sensor is capable of two output frequency ranges 0 to 20 kHz and 0 to 200 kHz. The 200 kHz output is used to ensure that

vibrations caused by the horn are recorded, since the 20 kHz output would cutoff any higher order harmonics that may have been generated. This sensor has a sensitivity of $0.1 \mu\text{m}$ when operated in the 0 to 200 kHz frequency range.

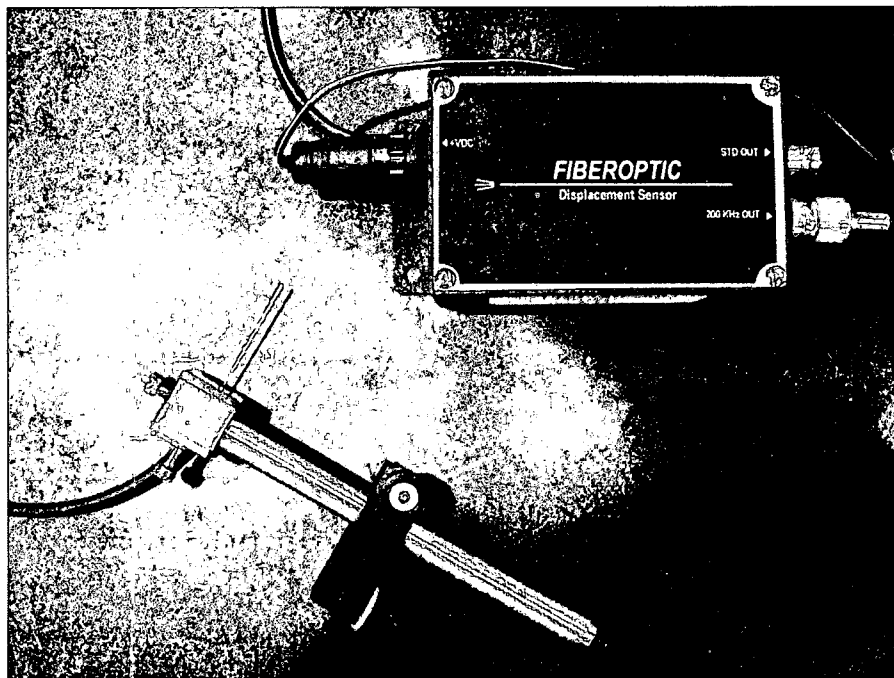


Figure 3: Fiber Optic Displacement Sensor

The output signal of the displacement sensor is passed through a Stanford Research Systems model SR560 low noise pre-amplifier. The pre-amplifier is set at a gain of one and is used as a 12 dB 100 Hz high pass filter. Filtering eliminates low frequency displacements that are introduced by the ambient environment. After passing through the pre-amplifier the output signal from the displacement sensor is recorded on a LeCroy 9310AM dual 400 MHz oscilloscope. The measurement of the peak to peak voltage of the signal allows

the displacement of the part or composite panel during excitation to be calculated from the response curves of the displacement sensor. A diagram illustrating the displacement measurement process is shown in Figure 4.

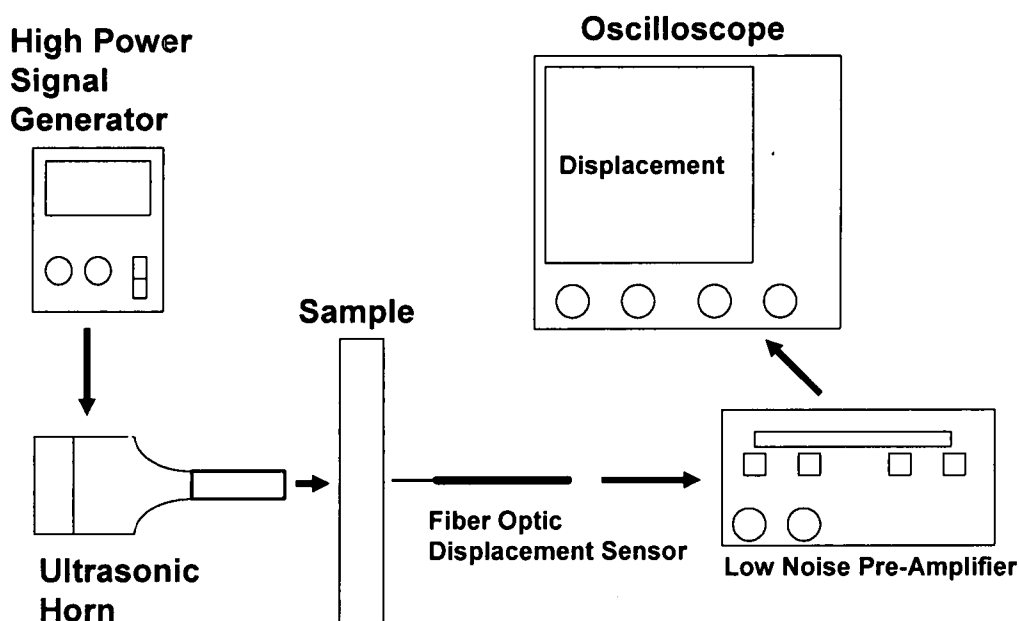


Figure 4: Diagram of Displacement Measurements

Temperature Increase Measurements

Maximum temperature rise of the composite is measured by an IR camera (item E in Figure 1). A Merlin Mid IR camera from Indigo Systems (now FLIR Systems) is used. The camera is capable of 60 frames per second and uses a 320 by 256 pixel InSb detector array to detect thermal energy variations. The

camera has a sensitivity of 0.025 °C. The array is cooled by an internal Stirling cycle engine. The camera has a crosshair measurement feature that allows the analog to digital (A/D) count information to be displayed for a particular pixel on the IR image. This A/D count information is related to the temperature at the location of measurement through an experimentally derived calibration curve. Using the calibration curve together with the A/D count reading before excitation and the maximum A/D count during inspection, the temperature increase in the composite is determined. The IR emissivity of the surface being measured is not a concern in this case as only relative temperature changes are being measured.

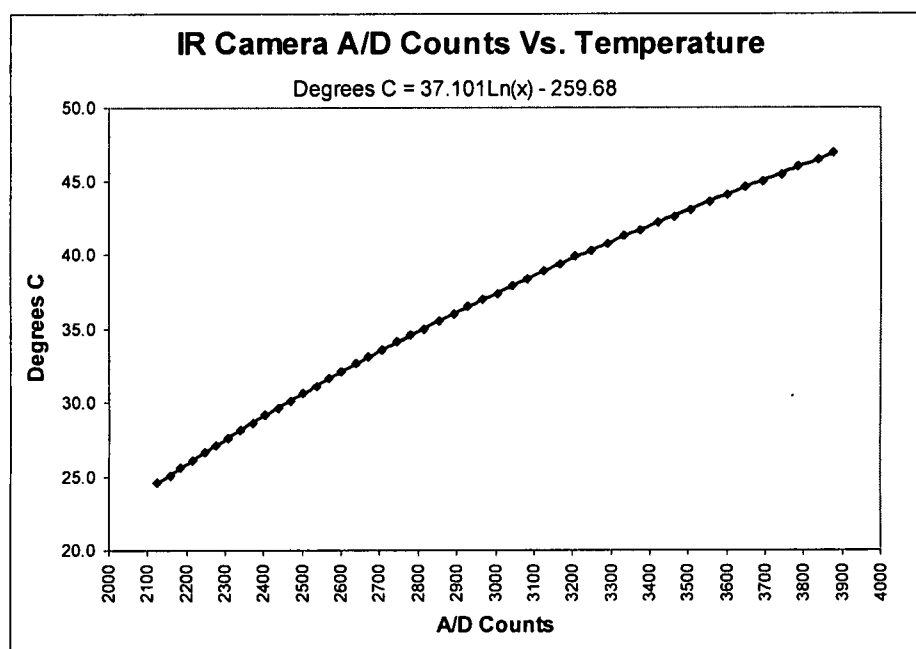


Figure 5: IR Camera Calibration Curve

Temperature measurements are taken at a series of excitations at each location to be inspected by varying the excitation amplitude in terms of percent of

the maximum power of the ultrasonic horn from 50% to 100% in 10% increments. This range is selected since it is the largest possible excitation range with the available power supply. Three measurements are taken at each amplitude of excitation for each location measured to insure consistent results. These three measurements are averaged to obtain one value for each amplitude. A diagram illustrating the temperature measurement process is shown in Figure 6. The displacement measurements cannot be collected at the same time as the temperature with the current set up. Therefore, the locations to be inspected are exposed to the series of excitations used during the temperature measurements another time. Three measurements of the displacements at each amplitude of excitation are also collected and averaged for each location measured. These two sets of data are combined to determine the relationship between the increase in temperature and the acoustic displacement.

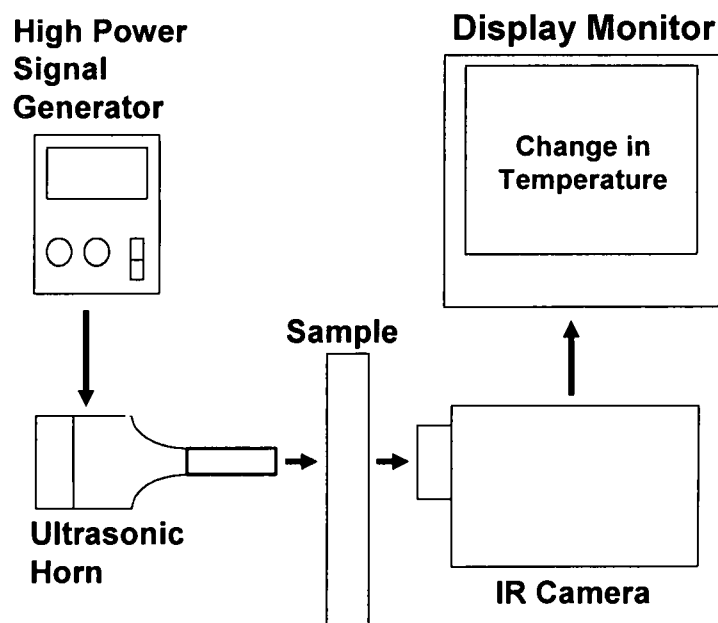


Figure 6: Diagram of Temperature Measurements

CHAPTER 3

COMPOSITE SAMPLES AND HEAT DAMAGE

Two types of heat damaged composite samples are examined. The first sample, which will be referred to as the Four Powers sample, has heat induced damage at several locations. The damage is generated by high intensity heat lamp exposures. The other samples, referred to collectively as the MLSA samples, are damaged by elevated temperature exposure in an oven. This creates uniform heat damage over the entire sample.

Four Powers Sample

The Four Powers group is an international group consisting of representatives from the United States, Great Britain, France and Germany that chooses certain NDE related issues of interest to all involved in order to combine resources and expertise to find a solution. The sample tested for this study is part of a set of two samples manufactured for the Four Powers NDE group. It is part of a round robin study to assess NDE techniques for detection of incipient heat damage under development by various national laboratories and companies available to the Four Powers group.

The sample in this study is manufactured by GE. It consists of Hexcel IM7 carbon fibers in Hexcel 8552 resin matrix. The lay up is $[0/+45/-45/90]_{2s}$ with 16 total layers. It also has a copper mesh laid over one side for lightning protection that is painted. Total sample thickness is approximately 2 mm. The sample is 180 mm wide by 260 mm in length.

The panel is heat damaged using a MICOR KIR spot radiator. This is a quartz lamp that has an output of 1000 W at the maximum input of 110 V. The reflector has a diameter of 100 mm. The radiator is located 47 mm from the panel. This results in a spot size of 15 mm in diameter. Thermocouples are used to monitor the temperature during exposure. One is located on the backside of the panel in the center of the exposure (ThC1) and the other thermocouple is also on the backside but it is 30 mm away from the center (ThC2). The panel is exposed to local heating at six locations. All exposures are done at an input voltage of 30 V, however the duration of exposure is varied by location. Locations are recorded as HS-1 to HS-6. Maximum temperatures recorded during exposure and the durations of exposure are listed in Table 1.

Location	Exposure Time, s	ThC1, °C	ThC2, °C
HS-1	180	171	97
HS-2	360	175	112
HS-3	540	185	106
HS-4	180	175	89
HS-5	360	175	98
HS-6	540	190	103

Table 1: Four Powers Sample Heat Exposure Data

Before the panel is tested by the non-contact thermo-elastic method it is characterized by available NDE methods. Photographs of both the exposed and unexposed sides of the panel are shown in Figure 7 and Figure 8. From the table one can see that the locations HS-1 and HS-4 are exposed for the least amount of time (180s) and the photographs show that these locations have the least amount of charring and no visible indications of delaminations. Locations HS-2 and HS-5 are damaged for 360s and they exhibit larger charring areas and there are visual indications of delaminations and loss of the matrix on the outer ply of the exposed side. HS-3 and HS-6 are both exposed for 540s. They exhibit significant differences in visual damage unlike the previous pairs of locations which show very similar visual features. HS-3 fits the trend of an increase in the size of the charred region and a larger region of outer ply matrix loss. HS-6 has a visually charred region that is the same size or only slightly larger than HS-2 and HS-5, and it has a smaller region of outer ply matrix loss than either of those two locations. It is possible that since composites are very anisotropic and have a high degree of inhomogeneity that this also causes them to react to heat exposure differently at different locations. The small rectangular area in the lower right corner of Figure 8 is a paper label. Ultrasonic (UT) C-scans of the exposed and unexposed sides with air-coupled 1.1 MHz transducers are also performed. The UT C-scan results are presented in Chapter 4.

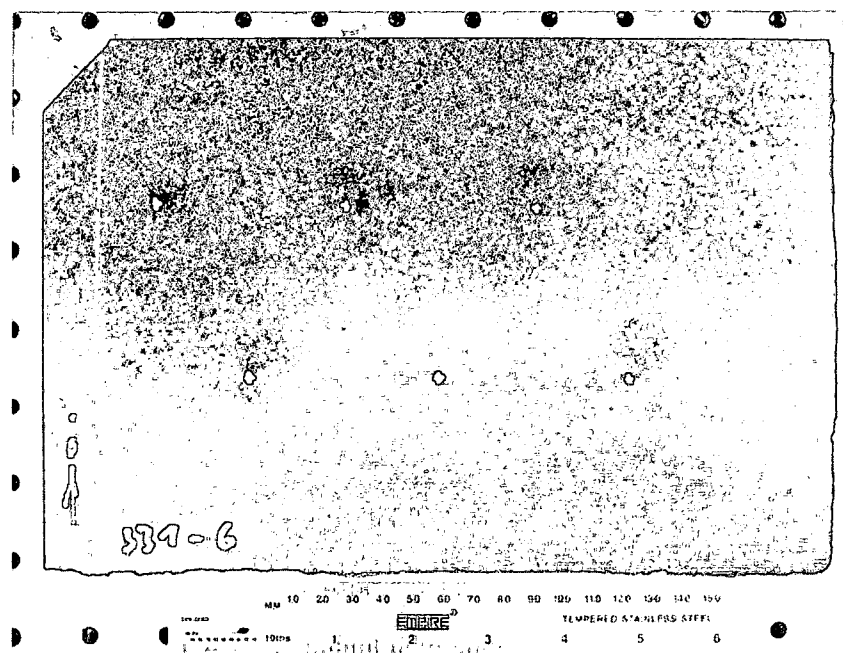


Figure 7: Four Powers Sample Exposed/Unpainted Side

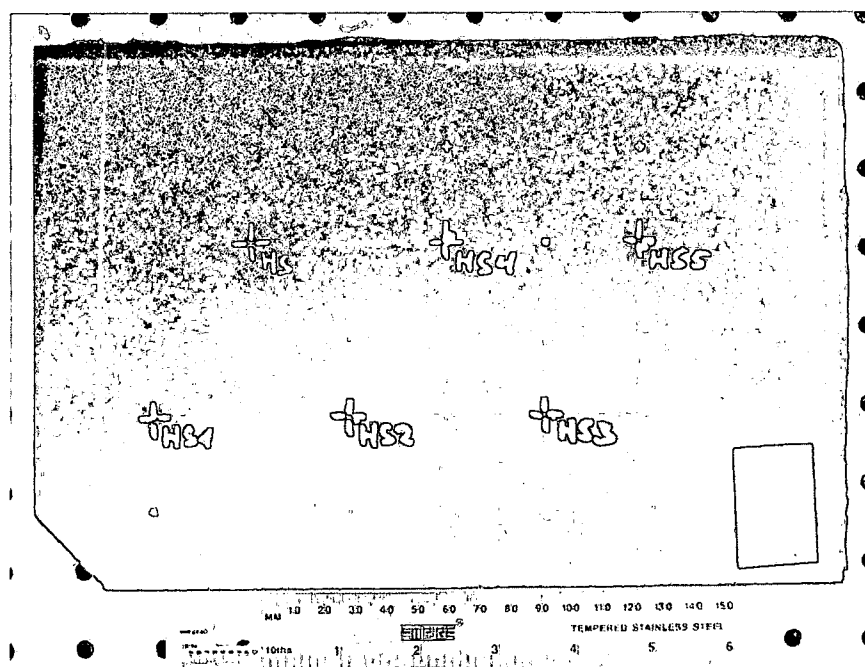


Figure 8: Four Powers Sample Unexposed/Painted Side

MLSA Samples

The other samples tested in this study are manufactured by the Materials Integrity Branch of the Air Force Research Laboratory. The samples in this study are numbered 11-5-P1-D and 11-5-P2-D. Both samples are cut from one large composite panel of Hexcel AS4 carbon fibers in Cyttec 977-3 resin matrix. The panel is manufactured with Cyttec pre-preg material using standard curing cycle instructions from the manufacturer. The lay up is $[0/+45/-45/90]_{2s}$ with 16 total layers. Total sample thickness is approximately 2 mm. The samples are approximately square measuring 150 mm on a side.

These samples are heat damaged by placing them a laboratory oven at 525°F (274°C) for 10 minutes in the case of sample 11-5-P1-D and 20 minutes for sample 11-5-P2-D. The temperature and times used here are based on incipient heat damage in composites studies performed by McShane on a similar fiber-matrix system [7]. The time and temperature combinations are selected to reduce the flexural strength the composite panels without inducing delaminations, i.e. to create incipient heat damage.

As in the case of the Four Powers panel optical images of the front (Figure 9) and back (Figure 10) of the samples after heat damage are taken. Water immersion UT C-scan images are also taken after heat exposure and thermo-elastic measurements to confirm that no delaminations are introduced either by the heat exposure or by the thermo-elastic measurements (shown in Chapter 4).

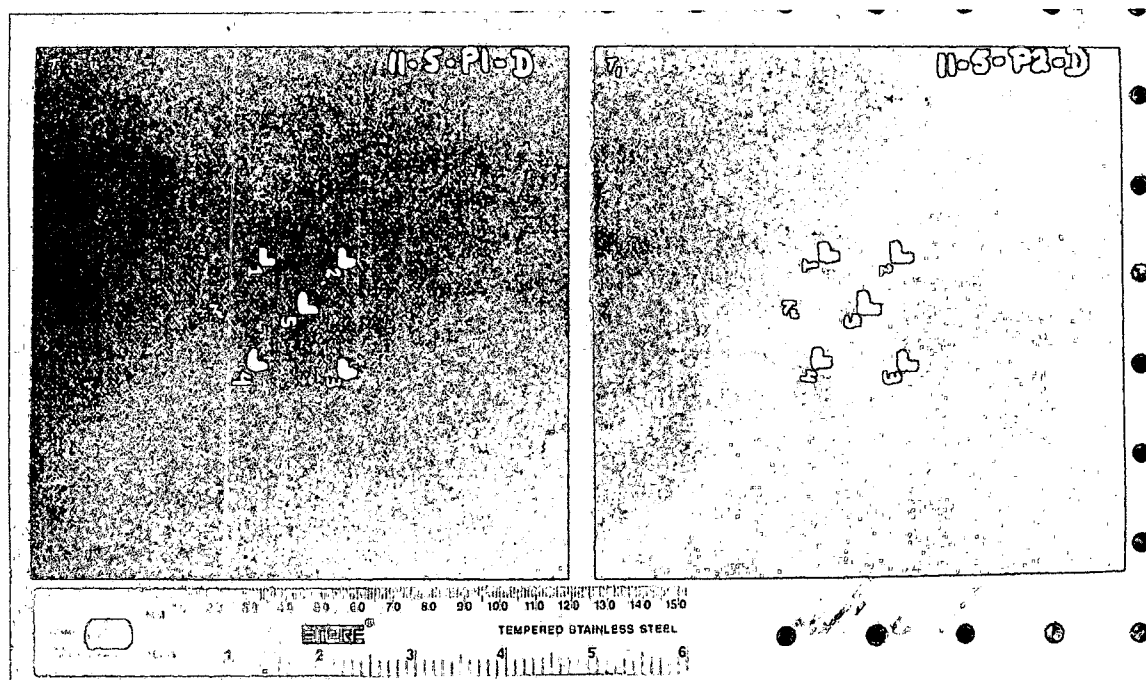


Figure 9: MLSA Panels Front/IR Camera Side

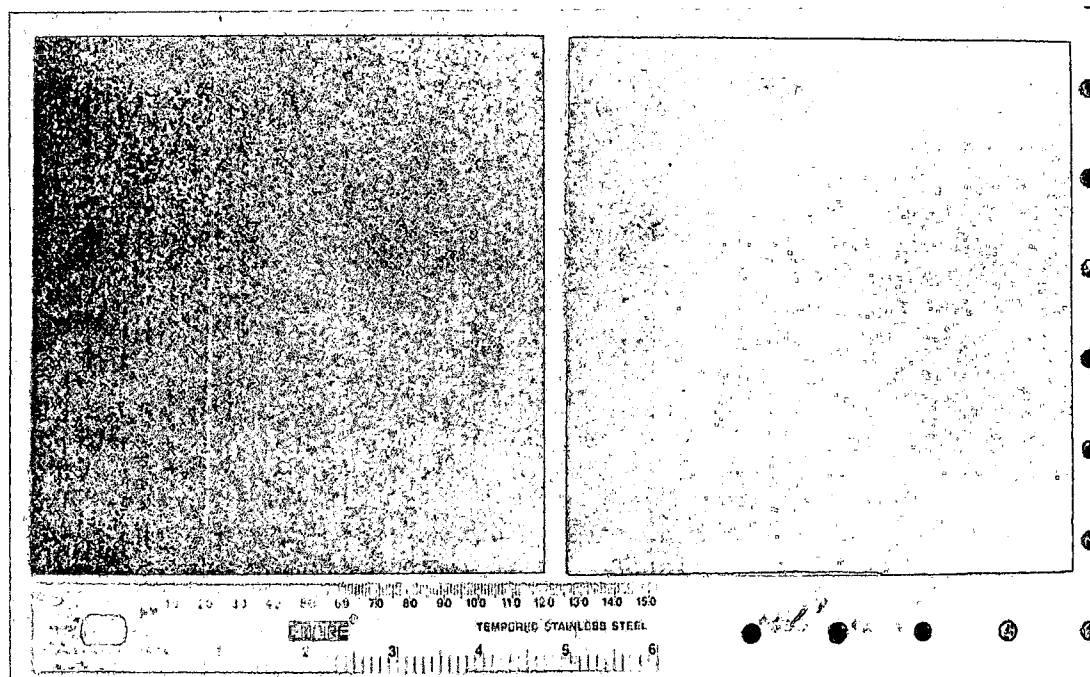


Figure 10: MLSA Panels Back/Ultrasonic Horn Side

CHAPTER 4

RESULTS AND DISCUSSION

In this chapter the results of the ultrasonic (UT) C-scans of the samples and the non-contact thermo-elastic measurements are shown and discussed. Conclusions from these measurements and potential future work are presented.

Ultrasonic C-scan Imaging

The Four Powers sample is ultrasonically imaged using air coupled transducers. Air coupled transducer is chosen for this sample because it exhibited visual indications of delaminations at locations HS-2, HS-3, HS-5 and HS-6. Traditional water immersion UT C-scanning would have allowed water to infiltrate the delaminations. The air coupled transducer scans yield much less depth information and less detail than immersion transducers. Therefore the scans are completed with the transmitting transducer on both sides of the sample. The MLSA samples are UT C-scanned using traditional water immersion transducers since they exhibited no visual indications of delaminations. Therefore these scans are performed on only one side of the sample.

Four Powers Sample

UT C-scans are performed using a Sonix UT scanning system with a 1.1 MHz air coupled transducer using the pulse-echo method. Scans are performed with the exposed side, and the unexposed side facing the transducer (Figure 11 and Figure 12). The small rectangular area in the lower right corner of Figure 12 is a paper label. The circular shaped indications at the location of HS-2, HS-3, HS-5 and HS-6 in the C-scan images are delaminations caused by the heat exposure.

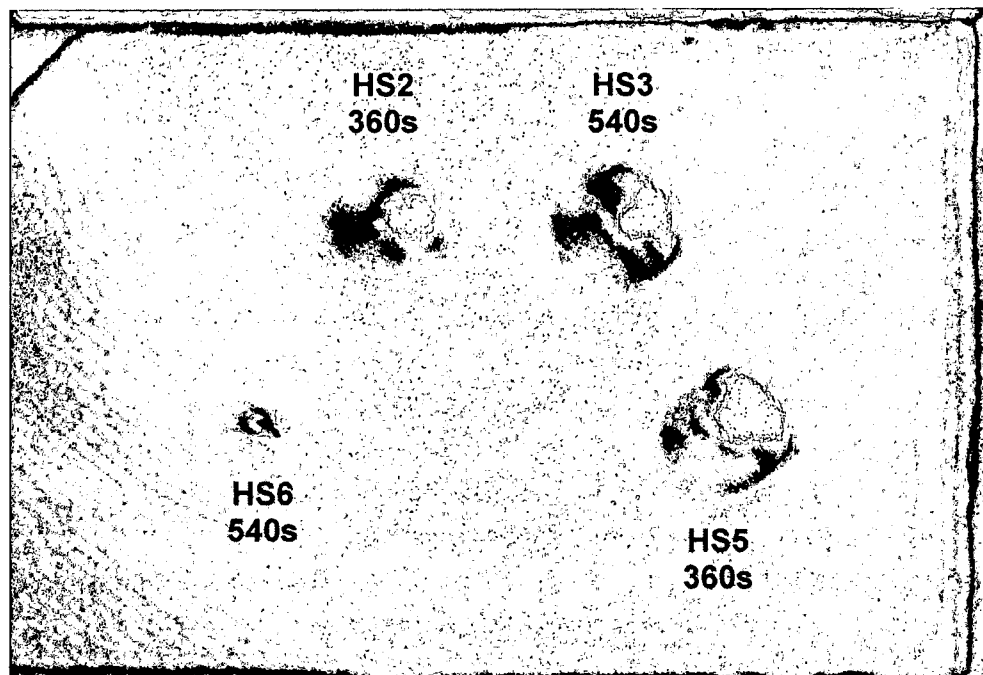


Figure 11: C-Scan Image: Four Powers Sample Exposed/Unpainted Side

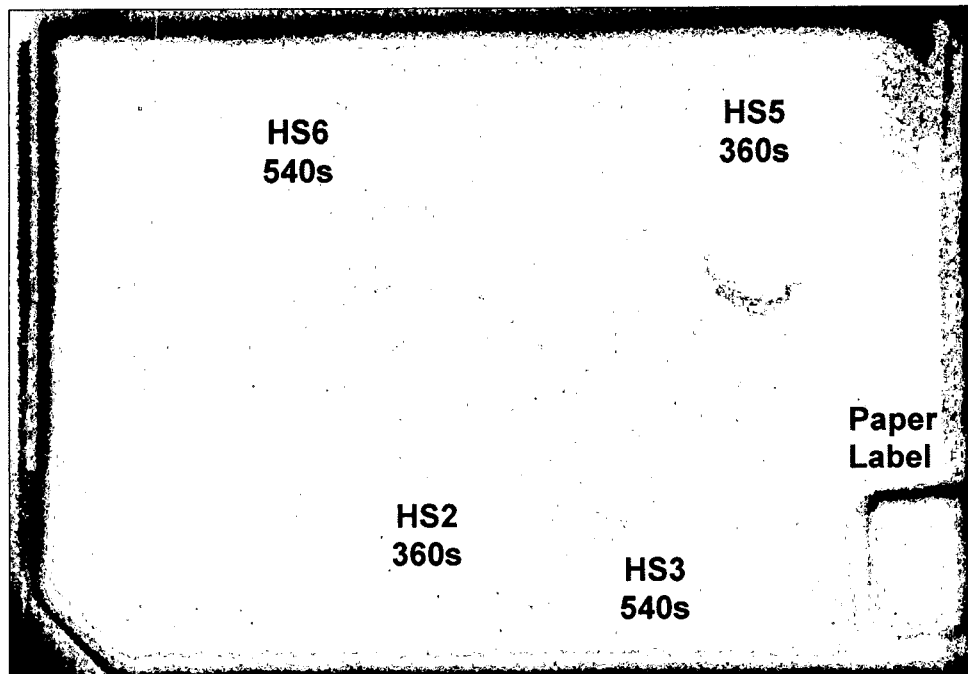


Figure 12: UT C-Scan Image: Four Powers Sample Unexposed/Painted Side

MLSA Samples

UT C-scans are performed using a Sonix UT system with a 5 MHz focused transducer using the pulse-echo method. Scans are performed with the backside (Figure 10) of the samples facing up. No gross delaminations are present in the C-scans. There are a few small circular defects in panel 11-5-P1-D (Figure 13) most of which can be attributed to surface imperfections, plus most of them are not within the area measured by the thermo-elastic technique at the center of the panel. Sample 11-5-P2-D (Figure 14) shows similar small circular defects, which can be correlated to small surface imperfections. This panel also has a

rectangular defect near the top edge of the scan image. Despite the size of the defect it does not fall within the region measured by the thermo-elastic technique and is therefore not addressed by this study.

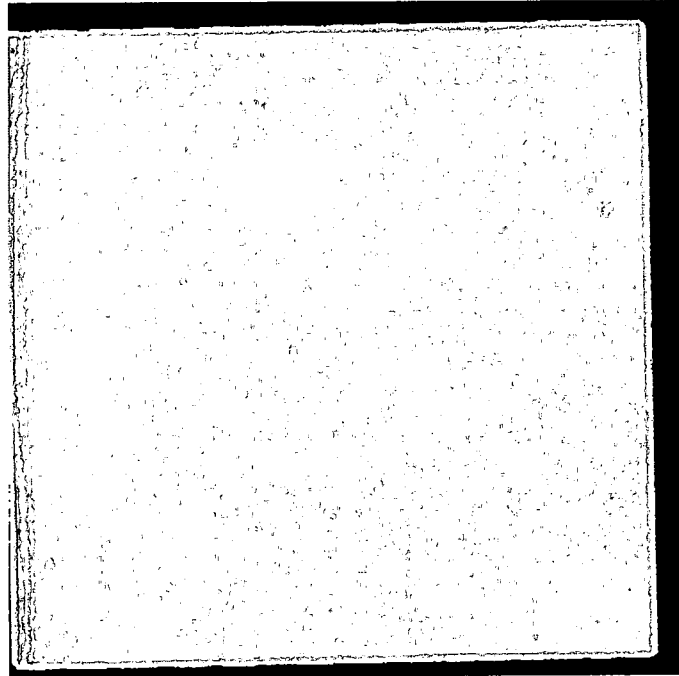


Figure 13: UT C-Scan Image: MLSA Panel 11-5-P1-D

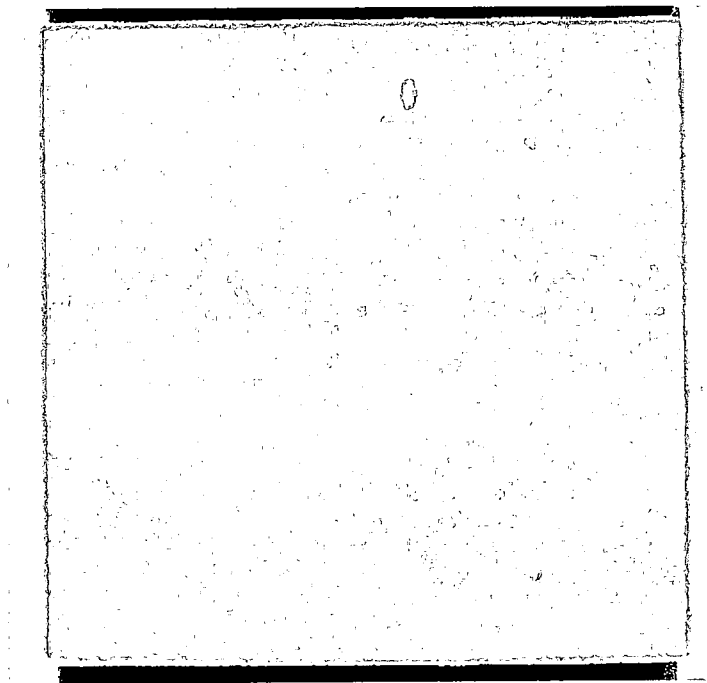


Figure 14: UT C-Scan Image: MLSA Panel 11-5-P2-D

Non-contact Thermo-elastic Measurements

Non-contact thermo-elastic measurements are conducted on the Four Powers panel and the two MLSA panels. The method of obtaining these measurements is the same in both cases. The trend of decreasing x^2 coefficient of the average temperature rise versus average displacement plot as amount of damage increases is shown. This trend is the same for the Four Powers sample and the two MLSA samples.

Four Powers Sample

Temperature measurements as a function of percent of maximum amplitude of the ultrasonic horn are taken at locations HS-4, HS-5, HS-6 and an undamaged location between HS-4 and HS-5. A series of excitations are used at each one of these locations consisting of amplitudes given in percent of the maximum power of the ultrasonic horn from 50% to 100% in 10% increments. Three measurements are taken at each amplitude for each location measured to insure consistent results. The three measurements for each amplitude and each location are averaged to give the mean value for each excitation amplitude at each location. An example of this is shown in Figure 15 using the data from the undamaged location. The displacement data is collected separately at the same locations for the same excitation amplitudes as the temperature measurements. The displacement is measured three times at each excitation amplitude for each location measured. The data is averaged in the same way as for the temperature data. The displacement data for the undamaged location is shown in Figure 16. As the displacement data and the temperature data are both a function of ultrasonic signal amplitude, these two parameters can be presented on the same graph. This is shown in Figure 17, which is a plot of the average temperature rise versus average displacement. The data for several different amounts of heat damage on this sample is shown in Figure 18.

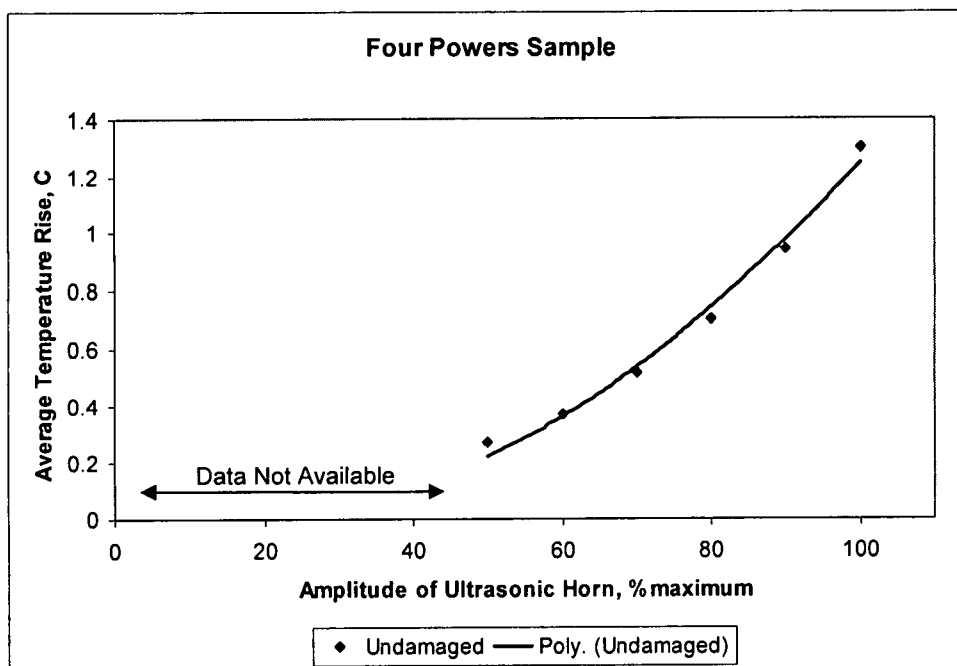


Figure 15: Four Powers Sample - Average Temperature Rise vs. Amplitude

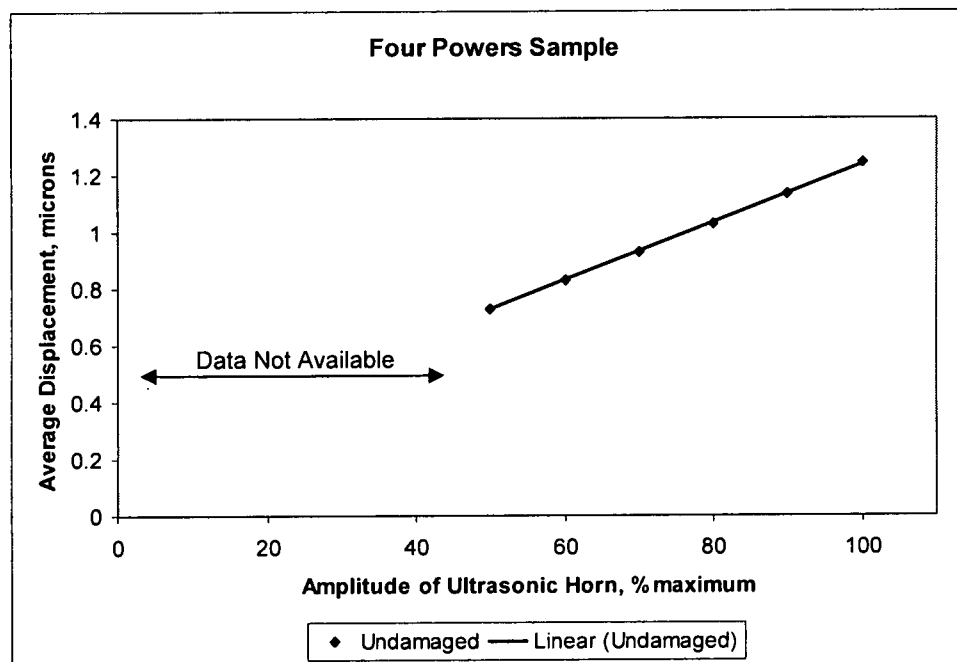


Figure 16: Four Powers Sample - Average Displacement vs. Amplitude

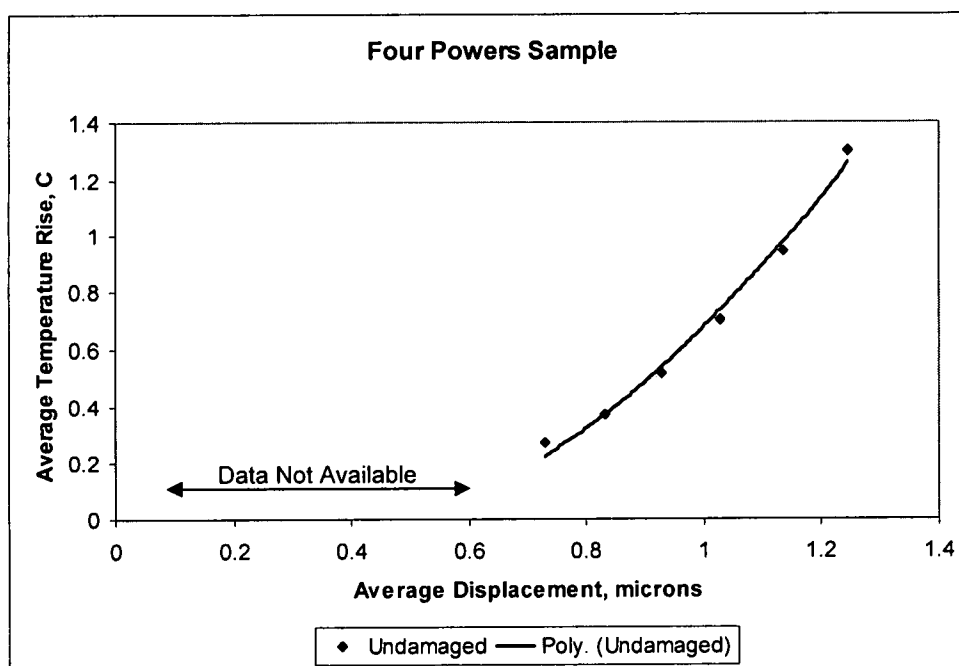


Figure 17: Four Powers Sample Average Temperature Rise vs. Average Displacement

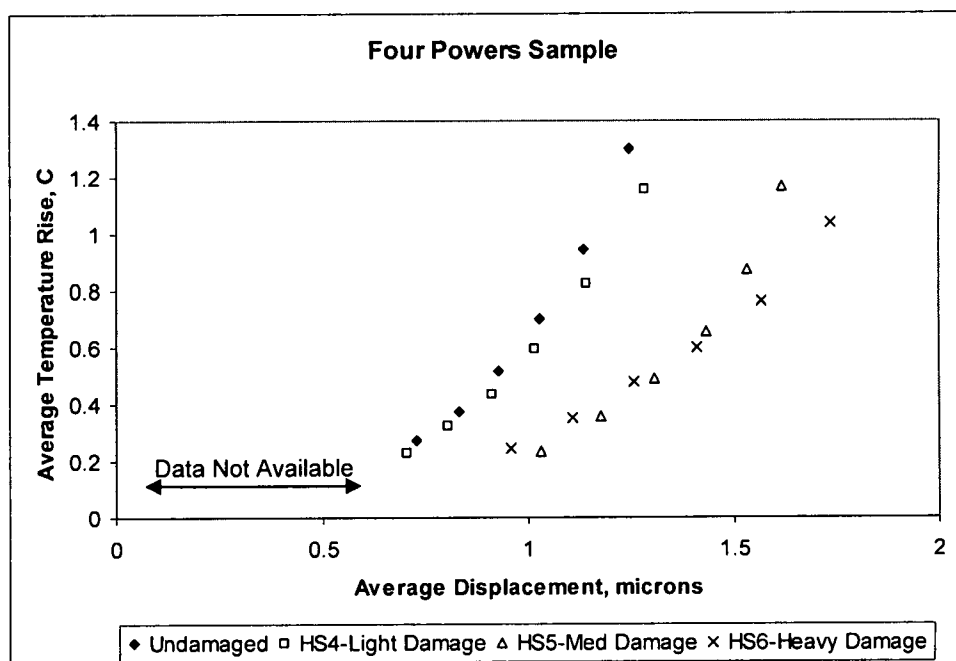


Figure 18: Four Powers Sample Average Temperature Rise vs. Average Displacement for Varying Amounts of Heat Damage

A quadratic fit is performed for each damage location measured. The x^2 coefficient determined for each damage locations and its comparison with the undamaged x^2 coefficient is displayed in Table 2. The analysis shows that the x^2 coefficient decreases as the amount of heat damage increases. For severe damage, HS-6, the x^2 coefficient changes by 71% compared to the undamaged location x^2 coefficient. For the least amount of heat damage measured, HS-4, the change is 29%. Thus the analysis of the data indicates areas of incipient heat damage. In addition this technique can distinguish between different amounts of incipient and heat damage. This is unique to this NDE technique.

Four Powers Location #	x^2 Coefficient	Difference from Undamaged	% Change
Undamaged	1.4		
HS-4	1.0	0.4	29
HS-5	0.8	0.6	43
HS-6	0.4	1.0	71

Table 2: Four Powers Sample: Comparison of x^2 Coefficients

MLSA Samples

To measure the temperature changes for different amplitudes of excitation for the MLSA samples, the same procedure as in the Four Powers sample is used.

Measurements are performed at five different locations on each sample. At each location three temperature measurements at each amplitude of excitation are performed and recorded. The acoustic displacement at each location is also measured three times for each amplitude at each location. To determine the relation between the temperature increase and the acoustic amplitude for the sample as a whole, the data from the five locations is averaged. This data is displayed in Figure 19 for sample 11-5-P1-D and in Figure 20 for sample 11-5-P2-D.

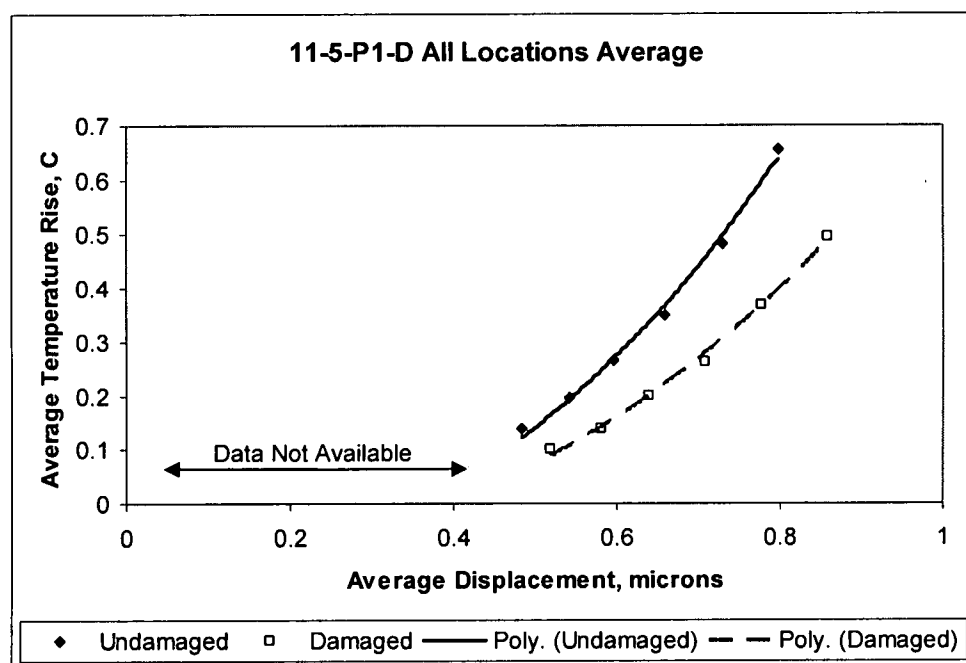


Figure 19: MLSA 11-5-P1-D: All Locations Average - Temperature Rise vs. Average Displacement

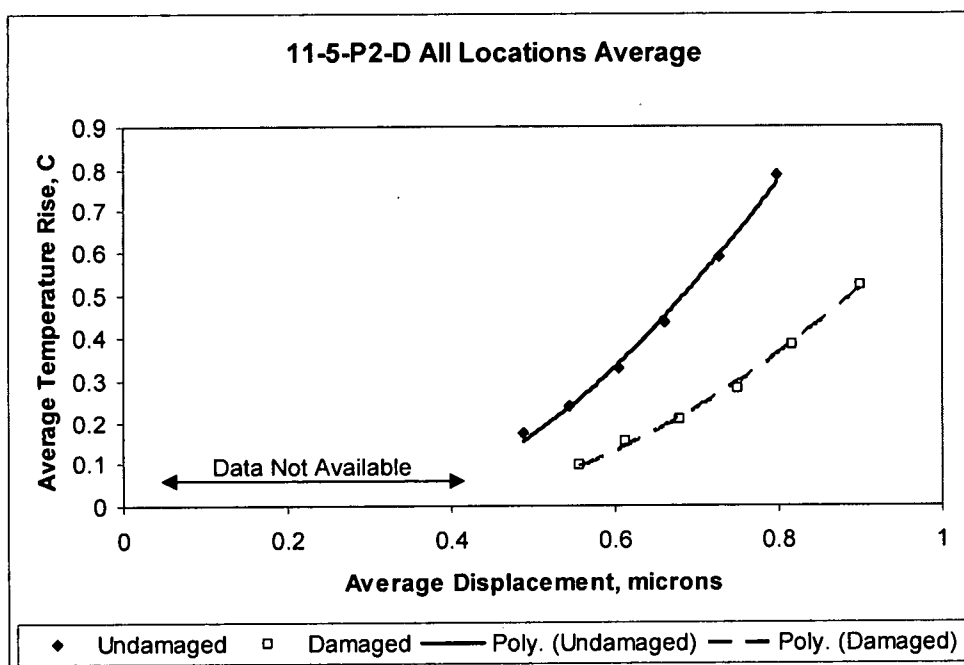


Figure 20: MLSA 11-5-P2-D: All Locations Average - Temperature Rise vs. Average Displacement Plot

A quadratic fit is performed on the data and is shown as the trend line in the previous plots. The x^2 coefficient is higher in both samples before subjecting them to controlled heat damage. These results are similar to those obtained on the Four Powers sample. One of the differences between the Four Powers sample and the MLSA samples is the magnitude of the scatter in the data. The MLSA samples had significant scatter in the acoustic displacement as well as the temperature increases from location to location. In spite of the scatter in the data, the change in temperature as a function of change in displacement of various amplitudes of ultrasonic excitation decreases with increasing heat damage. This is the same trend found in the Four Powers sample.

It is important to notice that the ultrasonic C-scans do not indicate any delaminations as a result of the heat damage while the thermo-elastic measurements show changes. The average x^2 coefficient changes by 29% after an exposure of 10 minutes at 525°F and by 43% in sample 11-5-P2-D that is exposed for 20 minutes at 525°F. Flexural strength testing of 11-5-P1-D shows a reduction in strength of 39% compared to an undamaged control sample. Sample 11-5-P2-D showed a 50% reduction in flexural strength. Flexural strength data [7] on a similar composite system (Fiberite unidirectional pre-preg consisting of IM6 fibers in 977-3 matrix resin with a $[(0/+45/-45/90)]_{2s}$ lay-up) that is heat damaged by oven exposure for 20 minutes at 525°F shows a greater than 50% reduction in flexural strength with heat exposure. The 43% change in the x^2 coefficient of sample 11-5-P2-D correlates to a greater than 50% reduction in flexural strength and 29% change in x^2 coefficient of sample 11-5-P1-D correlates to a 39% reduction in flexural strength.

Location #	Undamaged x^2 Coefficient	Damaged x^2 Coefficient	Difference	% Change
11-5-P1-D				
1	2.0	1.5	0.5	25
2	0.8	0.6	0.2	25
3	2.0	0.7	1.3	65
4	2.0	2.0	0.0	0
5	2.7	1.6	1.1	41
All Loc. Avg.	1.7	1.2	0.5	29
11-5-P2-D				
1	1.7	1.2	0.5	29
2	1.5	0.6	0.9	60
3	1.2	1.0	0.2	17
4	4.8	2.8	2.0	42
5	3.0	1.8	1.2	40
All Loc. Avg.	2.1	1.2	0.9	43

Table 3: MLSA Samples: Comparison of x^2 Coefficients

Discussion

The results of the Four Powers sample that is subjected localized heating at several locations as well as the MLSA samples that have been exposed to oven controlled heat damage of the entire panel at once show consistently that the change in temperature as a function of change in displacement of various amplitudes of ultrasonic excitation decreases with increasing heat damage. To obtain an understanding of the possible reasons for the changes in the x^2 coefficient, thermodynamic analysis of the thermo-elastic interaction in the composite materials is examined.

It is well known that the temperature of a material subjected to compressive load increases by a small amount and conversely when a material is subjected to tensile loading its temperature decreases [34]. During cyclic loading at low frequencies the temperature increases in the compressive portion and decreases in the tensile part. At low frequencies the average temperature remains the same because of the cancellation during the compression and tensile stages. On the other hand, when the cyclic loading frequency is increased, there will not be enough time for equalization and hence the mechanical energy is lost as thermal energy. This is known as thermo-elastic damping. The role of thermo-elastic damping has been studied extensively in the context of internal friction in materials with significant progress being made between 1940 and into the 1960s [35, 36]. The role of conversion of mechanical energy into heat and the loss of mechanical energy is studied through analysis of frequency dependence of mechanical damping.

The experimental configuration presented in this thesis allows the direct measure of the conversion of mechanical energy into heat. Thermodynamics is used effectively to evaluate thermo-elastic damping. Here the thermodynamics of deformed material is used to evaluate the change in temperature, following similar arguments.

The free energy of a deformed material can be written as described by Landau and Lifshitz [36]:

$$A = A_0(T) + A_1(T)\varepsilon_{ii} + \mu \left(\varepsilon_{ij} - \frac{1}{3} \delta_{ij} \varepsilon_{kk} \right)^2 + \frac{B}{2} \varepsilon_{kk}^2 \quad (1)$$

where $A_0(T)$ is the free energy per unit volume of the system at temperature T , μ is the shear modulus, B is the bulk modulus, and the strains in the material are represented by ε_{ii} , ε_{ij} , and ε_{kk} . The term $A_1(T)\varepsilon_{ii}$ is a function of temperature and for $T=T_0$ it is zero. For $|T - T_0| \ll T_0$ the free energy can be written as:

$$A(T) = A_0(T) - B\alpha(T - T_0)\varepsilon_{kk} + \mu \left(\varepsilon_{ij} - \frac{1}{3} \delta_{ij} \varepsilon_{kk} \right)^2 + \frac{B}{2} \varepsilon_{kk}^2 \quad (2)$$

where α is the coefficient of thermal expansion. The propagation of an acoustic wave and the deformation caused is adiabatic in nature. Hence the entropy remains constant during adiabatic deformation, thus:

$$\frac{\partial A(T)}{\partial T} = S(T) \quad (3)$$

Differentiating $A(T)$:

$$S(T) = S_0 T + B\alpha\varepsilon_{ii} \quad (4)$$

$$S(T) - S_0 T = B\alpha\varepsilon_{ii} \quad \text{or} \quad (5)$$

$$dS_0 = (B\alpha)d\varepsilon_{ii} \quad \text{or} \quad (6)$$

$$\int_{T_0}^T dS_0 = -B\alpha \int_0^{\varepsilon_{ii}} d\varepsilon_{ii} \quad (7)$$

$S_0(T)$ is the entropy of the solid at temperature T , when the volume of the solid is the same at temperature T_0 . Hence:

$$dS_0 = C_v \frac{dT}{T} \quad (8)$$

$$\int_{T_0}^T C_v \frac{dT}{T} = -B\alpha \int_0^{\varepsilon_{ii}} d\varepsilon_{ii} \quad (9)$$

$$C_v \ln\left(\frac{T}{T_0}\right) = -B\alpha \varepsilon_{ii} \quad (10)$$

For $\frac{T-T_0}{T} \ll 1$ and $\ln \frac{T}{T_0} \approx \frac{T-T_0}{T}$:

$$\frac{T-T_0}{T} = -\frac{B\alpha}{C_v} \varepsilon_{ii} \quad (11)$$

From Landau and Lifshitz, for an acoustic wave of frequency f , ε_{ii} can be approximated as [36]:

$$\varepsilon_{ii} = \frac{2\pi f}{V_L} u \quad (12)$$

where V_L is the longitudinal acoustic wave velocity in the material and u is the acoustic displacement. Substituting this into equation (11):

$$\frac{T-T_0}{T} = \left(-\frac{B\alpha}{C_v}\right) \left(\frac{2\pi f}{V_L} u\right) \quad (13)$$

In general $C_p \approx C_v = C$ in solids. For longitudinal wave propagation, B can be approximated by the Young's (elastic) modulus in the material, $B \approx E = V_L^2 \rho$.

Thus the change in temperature is:

$$\frac{T-T_0}{T} = 2\pi f \left(\frac{V_L \alpha}{C}\right) u \quad (14)$$

From this expression, it can be seen that the change in the temperature caused by an acoustic wave in a material is a function of the thermal properties (α and C_v) and the elastic property (V_L). Thus, it is a combined effect of the thermal and elastic properties of the material. Equation (14) shows that the temperature change is directly proportional to the amplitude of displacement. However, the experimental observation shows a quadratic behavior. The thermodynamic theory described here assumes the material is purely elastic in nature. The materials used in the experimental measurements are known to be visco-elastic. Under the influence of deformation the material may behave like a thermo-visco-elastic material rather than a simple thermo-elastic material. This might be one of the reasons for the discrepancy between the experiments and the simple thermodynamic theory. Further investigation is needed to clarify this point.

The majority of NDE techniques measure a single material property like elastic modulus, thermal conductivity, or electrical conductivity. The measurement of temperature in the experiments presented here is a measure of the combined thermal and elastic properties. The changes in the coefficient of x^2 observed, due to heat damage, in the measurements can be attributed to changes in both properties. It is believed that even though the changes in thermal or elastic properties may be small, the combined change in both properties might have a large variation due to heat damage.

The scatter in the x^2 coefficient data for the Four Powers and the MLSA samples could be attributed to a number of factors. One factor is the displacement measurements. Although the excitation frequency is 20 kHz, when acoustic waves propagate through the sample there is the possibility of generating other acoustic frequencies. For proper calculation of temperature changes, the displacements at the other frequencies need to be measured. In the present experiments the displacement amplitudes are measured only at 20 kHz.

The temperature and displacement measurements are acquired at a single point. These point measurements require precise alignment of the fiber optic displacement probe with center of the horn. It is possible that the ultrasonic horn excitation is not uniform cross its entire face. This would yield different temperature and displacement data depending on the location on the sample where the measurements are obtained. A technique to reduce this type of error would be to measure temperature and displacement data over the entire area of the horn face. This would reduce the effect of any alignment inconsistencies. In the case of the temperature data, this could be accomplished by recording the A/D count data for an area rather than a single point. For the displacement data, this could be achieved with a larger diameter fiber optic displacement probe or a capacitance probe.

The displacement sensor also must be aligned with the center of the horn, but it also must be perpendicular to the surface being measured. The surface also must be light reflecting and should be smooth. The displacement sensor is aligned with care through these experiments however alignment may not have been sufficiently precise to prevent scatter in the data. The sample is painted with silver paint to make it reflective. During alignment when everything is static this method showed no indication of any potential problems. The inherent surface roughness may have an effect during the measurements when the part is in motion. A possible solution to this would be to use a capacitance probe to measure the displacements in place of the fiber optic displacement probe.

Another possibility is that while the sample location under test is centered in the opening of the sample holder, the holder itself may not provide uniform and consistent clamping for each location. Great care is given to ensure as consistent sample mounting as possible. Further improvements in measuring displacement, temperature as well as fixturing of the sample are expected to improve the precision and accuracy of these types of measurements.

Conclusions

The concept of a non-contact thermo-elastic measurement technique is developed and evaluated for composite heat damage evaluation. The

instrumentation to measure the temperature change due to the conversion of acoustic energy into heat is developed. A relation between the change in the temperature in the material and amplitude of the input acoustic wave is established for different materials. This relationship is found to be sensitive to the amount of incipient heat damage in PMCs. A measure of the change in temperature as a function of change in ultrasonically induced sample displacement is capable of detecting visible heat damage, and incipient heat damage. Based on flexural strength testing of 11-5-P2-D and data from the literature a change in the measured x^2 coefficient of 43% can be correlated to a reduction of greater than 50% in flexural strength. Similarly from flexural strength testing of 11-5-P1-D a change of 29% in the measured x^2 coefficient could be correlated to a 39% reduction in flexural strength.

Future Work

To increase the accuracy of the measurements, a technique for measuring the displacements generated in the composite by the ultrasonic excitation is needed to allow for a larger stand off distance. This surface displacement measurement technique must be less affected by surface reflectivity and alignment. Increasing the dimension of the measurement area would also help to minimize the errors. Methods such as a laser interferometer or a capacitance probe are possible solutions. Likewise increasing the area over which the

temperature is measured during excitation would reduce measurement inaccuracies.

There is still much work that must be done to fully understand the properties being measured here. Microscopic analysis of the composites before and after the various amounts of heat damage should be performed to determine the extent of any cracking and determine the magnitude of any fiber-matrix degradation. Chemical analysis should be performed before and after heat exposure to quantify matrix changes. Mechanical testing should be performed before and after heat damage so that results of this technique can be correlated to a material property of interest, which will lead to a quantitative rather qualitative determination of heat damage. Computational Modeling of the thermo-elastic and thermo-visco-elastic effects and their changes with heat exposure would also be beneficial to the understanding of the properties being measured. It could also reduce the number of tests to be done by aiding in the identification of key data points.

To fully take advantage of this additional testing, a much more involved test matrix must be developed to study composite degradation with varying temperature and time exposure. This should be done with a design of experiments approach to minimize the number of tests that need to be performed while maintaining the statistical rigor for the measurements. This type of approach can lead to the establishment of the lower and upper thresholds for

detectable damage should they exist and a very good understanding of the parameters under which this technique is effective. Application of this technique to other materials should also be explored.

REFERENCES

1. Mangalgiri, P. D., "Polymer-matrix Composites for High-temperature Applications," Defence Science Journal, vol. 55, no. 2, pp 175-193, 2005
2. Strong, B. A., Plastics: Materials and Processing, 2nd ed., Prentice Hall, 2000
3. Mouritz, A. P., "Post-fire Flexural Properties of Fibre-reinforced Polyester, Epoxy and Phenolic Composites," J. Materials Science, vol. 37, no. 7, pp 1377-1386, 2002
4. Mouritz, A. P., "Fire Resistance of Aircraft Composite Laminates," J. Materials Science Letters, vol. 22, pp 1507-1509, 2003
5. Soutis, C., "Carbon Fiber Reinforced Plastics in Aircraft Construction," Materials Science and Engineering A, vol. 412, pp 171-176, 2005
6. Janke, C. J., et al, "Composite Heat Damage Assessment," Proceedings: Conference on Characterization and NDE of Heat Damage in Graphite Epoxy Composites, NTIAC, pp 77-96, 1993

7. McShane, H., et al. "Heat Damage Assessment for Advanced Composites," Proceedings: International SAMPE Symposium and Exhibition, vol. 42, issue 2, pp 890-903, 1997
8. Matzkanin, G. A., Hansen, G. P., "Heat Damage In Graphite Epoxy Composites: Degradation, Measurement and Detection: A State of the Art Report," NTIAC-SR-98-02, NTIAC, 1998
9. Matzkanin, G. A., "Nondestructive Characterization of Heat Damage in Graphite/Epoxy Composites: a State of the Art Report," Proceedings: Conference on Characterization and NDE of Heat Damage in Graphite Epoxy Composites, NTIAC, pp 9-26, 1993
10. Ng, S. J., Cramer, R. J., Mehrkam, P., "Characterization of IM7/8552 Polymer Composites Subjected to Heat Damage," 29th International SAMPE Technical Conference, vol. 29, pp 776-786, 1997
11. McShane, H. A., et al, "Heat Damage Assessment For Naval Aircraft Composites," NAWCADPAX-99-112-TR, Naval Air Warfare Center Aircraft Division, Patuxent River, MD, 1999

12. McShane, H. A., "Heat Damage Assessment in Naval Aircraft Composites" Overheated Composites Workshop, Dayton, Ohio, July 1997
13. Boltz, E. S., Johnson, R. I., Tiernan, T. C., "Mechanical Testing and NDE of Graphite-Epoxy Composites Exposed to Intense Fuel Fires," Overheated Composites Workshop, Dayton, Ohio, July 1997
14. Frame, B. J., et al, "Composite Heat Damage, Part 1. Mechanical Testing of IM6/3501-06 Laminates, Part 2. Nondestructive Evaluation Studies of IM6/3501-06 Laminates," ORNL/ATD-33, Oak Ridge National Laboratory, Oak Ridge, TN, 1990
15. Stanley, R. K., Moore, P. O., McIntire, P., "Nondestructive Testing Handbook 2nd ed., Vol. 9 Special Nondestructive Testing Methods," American Society for Nondestructive Testing, 2003
16. Davis, J. R., "Metals Handbook, Desk Edition, 2nd ed.," pp 31, ASM International, 1998
17. Armstrong-Carroll, E., Mehrkam, P. A., Cochran, R., "Characterization of Heat Damage in Graphite/Epoxy Composites," Composite Materials: Testing and Design (vol. 12), ASTM STP 1274, pp 37-55, ASTM, 1996

18. Haskins, J. F., "Thermal Aging," SAMPE Journal, vol. 25, no. 2, pp 29-33, 1989
19. Mehrkam, P. A., Armstrong-Carroll, E., "Detection of Heat Damage by Drift Spectroscopy," Proceedings: International SAMPE Symposium and Exhibition, vol. 38, issue 1, pp 217-225, 1993
20. Bray, D. E., McBride, D., "Nondestructive Testing Techniques," John Wiley and Sons, 1992
21. Collins, R., Mahon, J., "NDI for Heat Damaged Advanced Composites," Proceedings: Conference on Characterization and NDE of Heat Damage in Graphite Epoxy Composites, NTIAC, pp 53-68, 1993
22. Ong, P. S., "Backscattered X-rays for Nondestructive Evaluation," Proceedings: Conference on Characterization and NDE of Heat Damage in Graphite Epoxy Composites, NTIAC, pp 149-156, 1993
23. Lambrineas, P., Yeung, K. K., Finlayson, R. D., "Imaging of Burned Glass Reinforced Plastic (GRP) Using Compton Scattering," Proceedings: Conference on Characterization and NDE of Heat Damage in Graphite Epoxy Composites, NTIAC, pp 157-173, 1993

24. Fisher, W. G., et al., "Laser Induced Fluorescence Imaging of Thermal Damage in Polymer Matrix Composites," *Materials Evaluation*, vol. 55, no. 6, pp 726-729, 1997
25. Janke, C. J., et al., "Composite Heat Damage Spectroscopic Analysis: Part 1. Mechanical Testing of IM6/3501-6 Laminates, Part 2. Laser-Pumped Fluorescence Spectroscopic Studies on IM6/3501-6 Laminates, Part 3. Diffuse Reflectance Infrared Fourier Transform Spectroscopic Studies on IM6/3501-6 Laminates," ORNL/ATD-42, Oak Ridge National Laboratory, Oak Ridge, TN, 1990
26. Lindgren, E., "Personal Conversation," April 2006
27. Henneke, E. G., Reifsnider, K. L., Stinchcomb, W. W., "Thermography-An NDT Method for Damage Detection," *Journal of Metals*, vol. 31, no. 9, pp 11-15, 1979
28. Mignogna, R. B., et al., "Thermographic Investigation of High-Power Ultrasonic Heating in Materials," *Ultrasonics*, pp 159-163, July 1981
29. Favro, L. D., et al., "Infrared Imaging of Defects Heated by a Sonic Pulse," *Review of Scientific Instruments*, vol. 71, no. 6, 2000

30. Burke, M. W., Miller, W. O., "Status of VibroIR at Lawrence Livermore National Laboratory," Thermosense XXVI, Proceedings of SPIE, vol. 5405, pp 313-321, 2004
31. Mian, A., et al., "Fatigue Damage Detection in Graphite/Epoxy Composites Using Sonic IR Imaging Technique," Composites Science and Technology, vol. 64, pp 657-666, 2004
32. Mayton, D., Spencer, F., "A Design of Experiments Approach to Characterizing the Effects of Sonic IR Variables," Thermosense XXVI, Proceedings of SPIE, vol. 5405, pp 322-331, 2004
33. Perez, I., Davis, W. R., "Optimizing the Thermosonics Signal," Review of Progress in Quantitative Nondestructive Evaluation, vol. 22, pp 505-512, 2003
34. Biot, M. A., "Thermoelasticity and Irreversible Thermodynamics," Journal of Applied Physics, vol. 27, pp 240-253, 1956
35. Zener, C., "Elasticity and Anelasticity of Metals," University of Chicago Press, Chicago, 1948

36. Landau, L. D., Lifshitz, E. M., "Theory of Elasticity, 2nd ed., Pergamon Press, Oxford, 1970

R002588853